Available online at www.sciencedirect.com

ScienceDirect

Procedia Structural Integrity 44 (2023) 1925–1932

Structural Integrity Procedia

www.elsevier.com/locate/procedia

XIX ANIDIS Conference, Seismic Engineering in Italy

Innovative connections for steel-concrete-trussed beams: a patented solution

Alessia Monaco[a*], Salvatore Pagnotta[b], Piero Colajanni[b], Lidia La Mendola[b]

[a] *DAD – Politecnico di Torino – V.le Mattioli, 39 – 10125 Torino, Italy*
[b] *DI – Università di Palermo – Viale delle Scienze, Ed. 8 –90128 Palermo, Italy*

Abstract

The most recent design strategies welcome the adoption of innovative techniques for seismic energy input mitigation, aiming to achieve high dissipation capacity, prevent the structure from collapse and ensure the serviceability of the construction. Friction damper devices have been widely adopted in framed steel structures for decades, while their introduction in different structural types is still under investigation. This paper presents the outcomes of innovative research supported by the industry and conducted on beam-to-column connections of RC structures in which the beams are Hybrid Steel-Trussed Concrete Beams (HSTCBs) and the columns are classical RC pillars. An innovative solution, recently patented, has been found for the mitigation of the effects of seismic cyclic actions on small-sized beam-column joints, typically characterised by a large amount of longitudinal reinforcement due to the small effective depth of the beam. This paper collects the main featuring steps of the innovative research, which has led to the patented solution. The calculation procedure for designing the proposed connection is shown, and the validation through 3D finite element modelling is described. For the structural analysis of the joint, several monotonic and cyclic simulations have been carried out with the scope of investigating different design moment values. The finite element results proved that the patented solution is effective in preventing beam, column and joint from damage and it is suitable for exhibiting adequate dissipative capacity ensured by a flexural behaviour dominated by wide and stable hysteresis loops.

Keywords: Friction dampers; Hybrid steel-trussed-concrete beams; RC joints; Finite element models; Earthquake design.

* Corresponding author. Tel.: +39 011 090 4881; fax: +39 011 090 4881.
E-mail address: alessia.monaco@polito.it

2452-3216
10.1016/j.prostr.2023.01.246

1. Objective of the study and motivations

Innovative techniques for seismic energy input mitigation are increasingly adopted in multi-storey framed structures with the scope of achieving adequate dissipation capacity that prevents structural collapse with consequent loss of human lives. In particular, the scientific community is interested in devices able to absorb the whole seismic energy, avoiding the damage of the primary load-bearing structural elements and allowing the serviceability of the construction. This is also needed because of the extremely high economic costs that structural repair would lead to after a violent earthquake. Friction connections are widely adopted in steel structures for this scope; the use of friction devices in beam-to-column joints prevents the main structure from damage and limits the cracking of the panel zone thanks to the increase of the bending moment lever arm and the entity of the bond actions transmitted by the beam rebars, which reduce the shear forces in the joint (Francavilla et al. 2018; Tartaglia et al. 2017; Colajanni et al. 2016).

In consideration of this, the concept of friction dampers at beam-to-column joints of RC framed structures is developed in this study. The case study analysed is particularized to frames made with Hybrid Steel-Trussed-Concrete Beams (HSTCBs) and RC columns. This particular type of beam is semi-prefabricated with a steel truss welded on a bottom thin plate and upper longitudinal steel rebars while the concrete core is cast in situ. HSTCBs are used in civil and industrial buildings for more than thirty years and their mechanical performance must be evaluated for ensuring compliance with the capacity design criteria and achieving an adequate amount of seismic energy dissipation, particularly in the beam-to-column joints (Colajanni et al. 2018; Colajanni et al. 2017; Ballarini et al. 2017; Monaco 2016; Colajanni et al. 2016). The adoption of HSTCBs in seismic areas presents a weak point: these beams are often used to cover large spans with low depths and therefore a large amount of steel reinforcement is required within the joint panel zone, making both the ends of the beam and the joint potentially vulnerable to the effects that the earthquake cyclic action could induce in the structure, with a dramatic reduction of its dissipation capacity (Colajanni et al. 2016).

The paper presents the main steps developed by the Authors, with the support of the industry, which led to a patented solution of friction device for HSTCB-column joints (Colajanni et al. 2021a,b; Colajanni et al. 2020; Colajanni et al. 2019). Specific design criteria are defined for the dimensioning of the device and, successively, the performance of the proposed solutions is validated through Finite Element (FE) models.

2. Calculation criteria

The concept of the friction connection placed in the joint between HSTCB and RC-column is based on the presence of steel members which act as rotation centre on the top of the connection, a system of three steel plates in contact with each other by means of friction bolts on the bottom of the connection; thus, both top and bottom steel profiles are connected by means of ad-hoc devices to the RC-column and to the hybrid beam in order to create the friction damping system.

The friction connection is designed starting from the design bending moment value M_d which activates the slippage of the system; the scope of the design procedure is avoiding the slip of the device at the serviceability limit state and allowing the dissipation under seismic events by means of the sliding. Therefore, the geometry of the device needs to be set through an iterative procedure aimed at the detection of the best internal lever arm value z_i for every i-th proposed solution (with i = 1, 2, 3 for solution A, B and C respectively). For conducting the feasibility study, an arbitrary value of M_d=110 kNm is assumed. This value is compatible with the hogging moment strength of the beam belonging to the subassembly, M_{Rd}=165 kNm, and calculated assuming an overstrength factor equal to 1.5. Finally, the friction damper is designed to withstand a sliding force $F_{d,i}$ figured as:

$$F_{d,i} = \frac{M_d}{z_i} \tag{1}$$

The number of preloaded bolts used is $n_{b,i}$ of area $A_{res,i}$ and ultimate strength $f_{ub,i}$. The preloading force $F_{pc,i}$ of each bolt according to Eurocode 3 (2005) is equal to:

$$F_{pc,i} = 0.7\, f_{ub,i} A_{res,i} \tag{2}$$

and the code-compliant slip resistance of the connection $F_{s,Rd,i}$ is calculated as:

$$F_{s,Rd,i} = k_s n_{b,i} n_s \mu F_{pc,i} / \gamma_{M3} \tag{3}$$

In Eq. (3), k_s and γ_{M3} are coefficient introduced in the design formula with the aim of preventing the sliding of the device until the ultimate limit state and therefore they are assumed equal to 1 in the current study. The terms n_s and μ represent the number of friction planes and the slip factor, respectively. In this study, all proposed solutions have n_s=2 and μ =0.4 is assumed.

Concerning the preload, several studies in the literature show that its value decreases progressively due to creep phenomena (Ferrante Cavallaro et al. 2018) and therefore the design preloading force $F_{pc,d,i}$ to be adopted should be contained in the range between 30%-60% of the code-compliant value of Eq. (2). In the present study, the ratio between effective and code-consistent preload is assessed through the coefficient $t_{s,i}$, which can be calculated as the ratio between design sliding force (Eq.(1)) and code-compliant slip resistance (Eq.(3)):

$$t_{s,i} = \frac{F_{d,i}}{n_{b,i} n_s \mu F_{pc,i}} \tag{4}$$

Therefore, the effective design value of preload will be assessed as:

$$F_{pc,d,i} = t_{s,i} F_{pc,i} \tag{5}$$

Based on Eq. (4), the parameter $t_{s,i}$ represents the stress level of each preloaded bolt and, therefore, the design procedure allows the diameter of the preloaded bolts to be easily changed, providing the same preloading force with a different stress level. Concerning the dimensions of the slotted holes, they are designed according to the displacement demand of the structure. Finally, the steel members that make the upper and lower connection to the beam and the column are calculated assuming that they have to withstand to the horizontal and vertical components of the design sliding force of Eq. (1) amplified by the overstrength factor.

3. The design solutions

Several solutions have been conceived in order to achieve the goal. In the next sections, three proposals will be shown, namely:

- solution A, i.e. friction device endowed with a hinged connection and crossed slotted holes;
- solution B, i.e. friction device equipped with a T-stub, curved slotted holes and shaped concrete section of the beam;
- solution C, i.e. friction device with shaped T-stub, curved slotted holes and perfobond connectors.

3.1. Solution A: device with crossed slotted holes

The scheme of the connection proposed as Solution A is represented in Fig. 1. On the top, there is a pin connection that makes the centre of rotation C_1 of the system. The bottom connection is made of two lateral steel angles connected with a central plate by means of six M16 class 10.9 bolts ($A_{res,1}$ = 157 mm^2; $f_{ub,1}$ = 1000 MPa). Both steel angles and central plate are endowed of slotted holes in the vertical and horizontal direction, respectively. The cross-section of the beam is 250×300 mm; the internal lever arm results z_1 = 399 mm and the angle between the beam axis and the

point of application of the sliding force is $\alpha_1 = 61°$. Therefore, in this solution, $F_{d,1} = 275.7$ kN; $F_{pc,1} = 109.9$ kN; $t_{s,1} = 0.523$; $F_{pc,d,1} = 57.5$ kN.

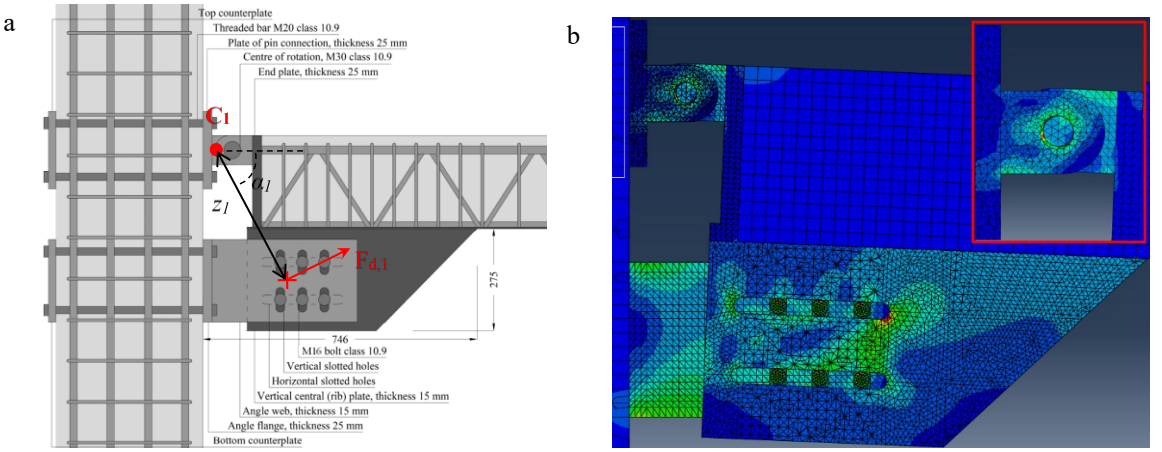

Fig. 1. Solution A: crossed slotted holes: (a) general scheme (dimensions in millimetres); (b) mesh of the FE model.

3.2. Solution B: device with curved slotted holes

The conception of the damping device is depicted in Fig. 2. Five bolts collocated on two rows are used and curved slotted holes are designed, with rotation centre C_2 indicated in the same figure. This system presents two main differences with respect to the previous one: on the bottom, vertical and horizontal holes are replaced by curved slotted holes while, on the top, the pin connection is substituted by a bolted connection with T-stub and C-shaped steel profile. More in detail, the curved geometry of the holes of the lower central plate allows the device to rotate keeping the bolts in their initial position even during the rotation; moreover, the cross-section of the T-stub web is made weaker by means of two 20 mm diameter holes aimed at favouring the activation of the centre of rotation of the system by means of a plastic hinge. A series of studs with variable inclination are introduced for increasing the stiffness between the concrete core of the beam and the central plate with curved slotted holes.

The preloaded bolts in the friction central connection are M18 class 10.9 ($A_{res,2} = 192$ mm^2; $f_{ub,2} = 1000$ MPa). In this case, the angle $\alpha_2 = 68°$ and the internal lever arm is $z_2 = 380$ mm. Therefore, in this solution, the following design parameters are calculated: $F_{d,2} = 289.5$ kN; $F_{pc,2} = 134.4$ kN; $t_{s,2} = 0.538$; $F_{pc,d,2} = 72.3$ kN.

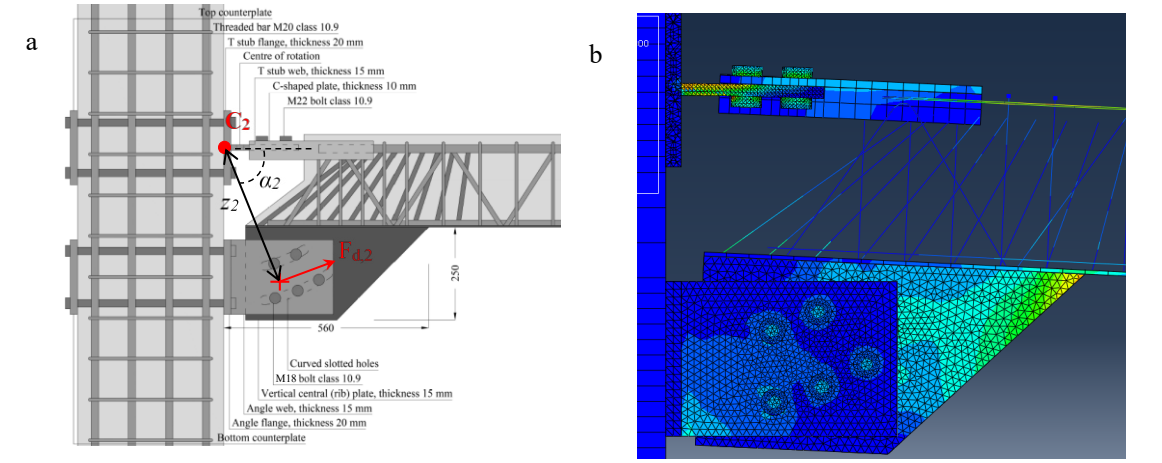

Fig. 2. Solution B: curved slotted holes: (a) general scheme (dimensions in millimetres); (b) mesh of the FE model.

3.3. Solution C: device with curved slotted holes and perfobond connectors

The third solution is represented in Fig. 3. One of the main differences with Solution B consists in the extension of the central plate with curved slotted holes throughout the beam; this vertical plate is then welded on the top to a horizontal plate that hosts the connection to the T-stub and the longitudinal top reinforcement of the beam, the latter made by coupled rebars welded on such horizontal plate. Moreover, both vertical and horizontal plates are equipped with slotted holes useful to make a so-called PerfoBond Connector (PBC), which is a type of shear connection used in steel-concrete composite structures. In the proposed solution, the concrete dowel action which develops in the PBC provides the shear resistance of the connector and the elongated holes on the top plate favour the proper pouring of concrete during the casting. A standard bolted connection is adopted for the T-stub, whose web middle cross-section is reduced in order to favour the formation of the plastic hinge, which acts as the centre of rotation of the system. Vertical studs are welded to the top plate of the PBC and the bottom plate of the steel truss to make the two parts connected; finally, the steel angles of the lower part of the device are characterized by a variable cross-section with the aim of improving the stiffness of the connection of the system to the column.

Five M20 class 10.9 bolts on two rows are used in the central plate ($A_{res,3}$ = 245 mm^2; $f_{ub,3}$ = 1000 MPa). In this case, the internal lever arm and its slope with respect to the beam axis are z_3 = 374 mm and α_3 = 68°, respectively. Therefore, for Solution C, the following design parameters are found: $F_{d,3}$ = 294.12 kN; $F_{pc,3}$ = 171.5 kN; $t_{s,3}$ = 0.429; $F_{pc,d,3}$ = 73.5 kN.

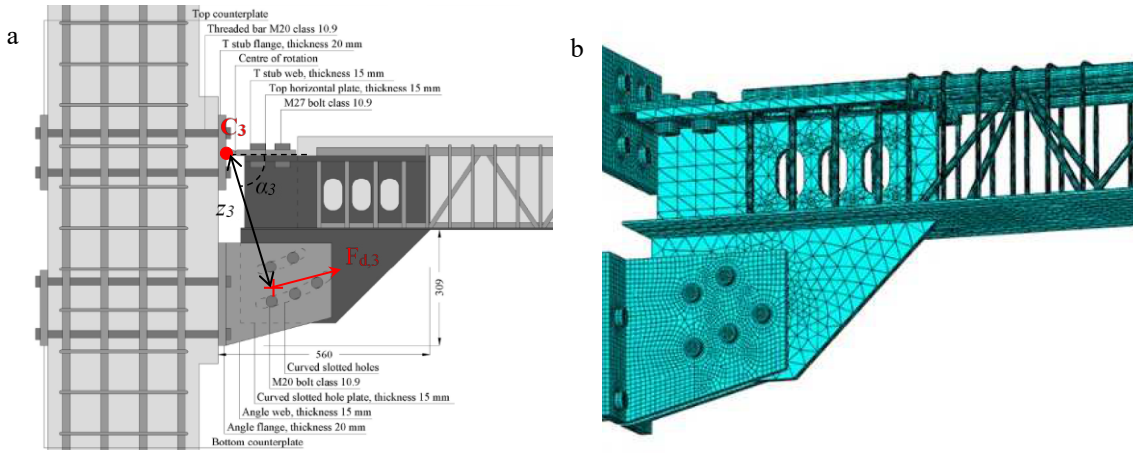

Fig. 3. Solution C: curved slotted holes and perfobond connectors: (a) general scheme (dimensions in millimetres); (b) mesh of the FE model.

4. Finite element analysis: modelling and results

The Finite Element (FE) model of all cases is representative of the behaviour of an exterior beam-to-column joint in which the cross-section and length of the members are 300×400 mm and 3 m for the column, while 250×300 mm and 2.5 m - 2.6 m - 2.73 m for the beam, the latter respectively for the models of Solution A, B and C. In the first two cases, the column is constrained at its top and bottom ends by hinges and a vertical displacement is applied at the beam tip; in the third case, the displacement is applied on the bottom end of the column in the horizontal direction (parallel to the beam axis) and a pre-compression axial load is applied to the RC column.

The FE models explore the response of the system under both monotonic and reversed cyclic loading with the scope of comparing the mechanical performance of each proposed solution, highlighting their main strengths and weaknesses.

4.1. Model A

The model developed for the validation of the first solution (Model A) assumes that all members behave in the elastic regime and, for simplicity, neglects the reinforcement details of both RC column and HSTCB, just focusing on the mechanism of the friction device. Two analyses are performed: Model A.1 is a monotonic analysis with vertical displacement up to 240 mm in the downward direction; Model A.2 is a cyclic analysis with displacement in the range ±100 mm.

Fig. 4a reports the moment-rotation diagram of Model A.1. Several phases are recognised during the whole analysis; in particular, the transition between phases 1 and 2 (i.e. linear elastic and plastic behaviour, respectively) indicates the step of the analysis in which the sliding force is achieved and the device starts rotating. However, because of the clearance between the shank of the pin and its plates, the rotation is still not exactly centred in the pin. This will happen slightly later, from phase 4, when the bending moment of the connection is approximately equal to the design value of 110 kNm. During the fifth phase, several jumps are recognised in the diagram, due to the clearance between the bolt shanks and their slotted holes in the friction plates. From phase 6, the system exhibits a new configuration in terms of stiffness, achieving design rotation capacity beyond the range of interest of the current connection. The cyclic analysis result also in terms of moment-rotation diagram, reported in Fig. 4b, confirms the negative effects of the clearance around the pin connection that causes the two sub-horizontal branches (included in the dashed rectangles in the figure), which represent the resistance provided by the friction plates when the pin moves inside the hole before finding the contact. This peculiar behaviour affects the stiffness of the system as well as its dissipation capacity.

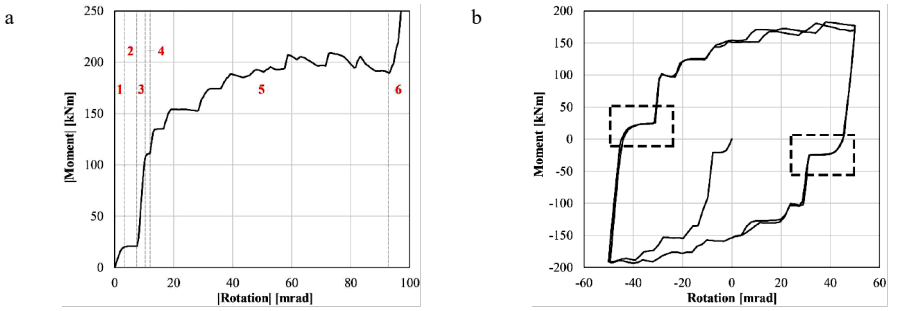

Fig. 4. Moment-rotation curve of (a) Model A.1; (b) Model A.2.

4.2. Model B

The model of the second solution (Model B) considers the material non-linearities. More in detail, the behaviour of the concrete is modelled by the Concrete Damaged Plasticity (CDP) model assuming the compressive stress-strain relationship by Saenz (1964) and the tensile response suggested in CEB-FIP Model Code (2010) in terms of fracture energy. The concrete compressive strength is f_c = 25 MPa, the elastic modulus E_0 = 28960 MPa, the tensile strength f_t = 2.56 MPa and the fracture energy G_F = 0.13 N/mm. The behaviour of the steel is modelled by means of an elastic-perfectly plastic stress-strain curve. In detail, the rebars are made of steel grade B450C while the constructional steel is S355. In both cases, the elastic modulus is E_s = 210000 MPa.

A detailed contact modelling has been implemented: perfect bond (embedded constraint) between the beam reinforcement and the concrete; pure sliding (frictionless contact property) between the bottom plate of the trussed beam and the concrete as well as between the C-shaped profile and the concrete; welds (tie constraint) between the bottom plate of the trussed beam and all inclined and vertical stirrups as well as between the C-shaped profile and the longitudinal rebars of the beam; friction contact property (by penalty method) between the friction shims. All normal contacts are rigid (hard contact property).

Monotonic (Model B.1) and cyclic (Model B.2) analyses are performed to simulate the condition of sagging and hogging bending moment. The cyclic analysis is conducted in the displacement range of ±100 mm. Moreover, analyses with different preload in the bolts have been performed with the aim of simulating the behaviour of the system for two

different design moment values, i.e. M_d and $1.5M_d$, 1.5 being the overstrength factor. The results of the simulations are reported in Fig. 5. In particular, Fig. 5a shows a trilinear behaviour in which, after the initial elastic phase in which no sliding occurs, an almost perfectly-plastic branch develops when the system starts sliding and the upper T-stub faces the plasticization which causes a slight translation of the centre of rotation designed. In the third phase, the design displacement limit is overcome. The cyclic response reported in Fig. 5b shows that the system behaves according to the design hypotheses, i.e. similar response for positive and negative bending moment and no significant damage during the loading-unloading phases.

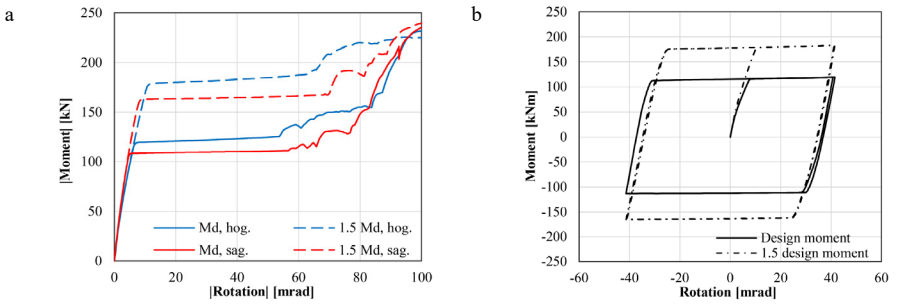

Fig. 5. Moment-rotation curve of (a) Model B.1; (b) Model B.2.

4.3. Model C

The third proposed model (Model C) simulates the last solution. In this case, the model is more detailed in terms of material properties and contact modelling. As regards materials, the concrete is modelled again with the CDP approach with the difference that, in this case, the concrete compressive strength assumed is f_c = 30.31 MPa and the elastic modulus is E_c = 30683 MPa. The steel grade of the beam reinforcement is B450C while S355 steel class is used for construction steel. However, for both reinforcement, steel members and bolts, multi-linear stress-strain relationships are adopted, which consider the hardening phases and the rupture of the material (D'Aniello et al. 2017, Yun and Gardner 2017). As regards contacts, the classical bond model by Eligehausen et al. (1983) is adopted at the interface of the reinforcing rebars of the beam and the concrete. The analyses are performed for three values of the design bending moment, i.e. 0.5 M_d, M_d and 1.5 M_d. Figure 6 reports the results of the monotonic and cyclic analyses. The cyclic tests are conducted by adopting the displacement history reported in Fig. 6c. The results of the monotonic analyses show that this connection has adequate stiffness to ensure that the centre of rotation of the system is prevented by any shifting. As a matter of fact, the third branch of the curve, which represents the phase in which the bolt shanks go into contact with the profile of the curved slotted holes, starts for a rotation of about 70 mrad for almost all analyses. This rotation value is much higher than the design one of 50 mrad. Figure 6b shows that the hysteresis loops are wide and stable as required by the design and the response of the system is proportional by varying the bolt preload.

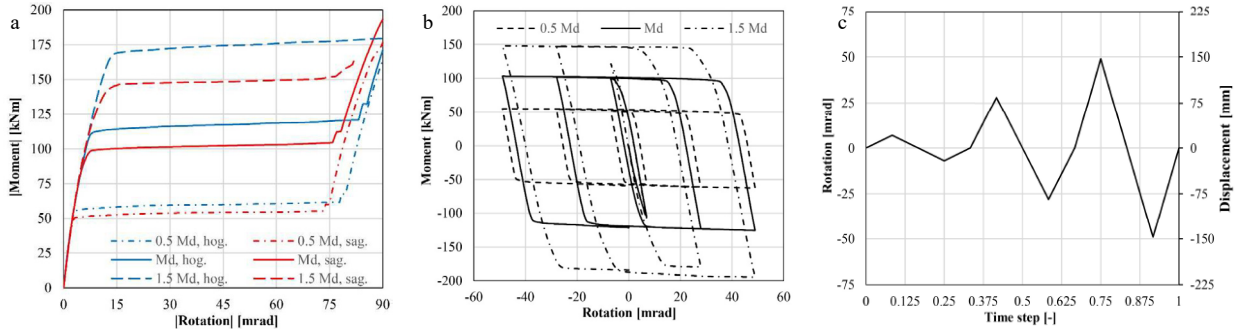

Fig. 6. Model C: (a) monotonic moment-rotation curve; (b) cyclic moment-rotation curve; (c) displacement history of the cyclic tests.

5. Conclusions

This research proposes three different design solutions of dissipative connections to be adopted in beam-to-column joints of seismic framed structures characterized by the presence of HSTCBs and RC columns. In Solution A, the friction device is made with three friction shims with vertical and horizontal slotted holes, preloaded bolts and pin connection on the top as centre of rotation. This first tentative solution shows a pinching effect in the cyclic response, caused by the clearance of the pin connection, and additional resistance of the dissipative device, caused by the shifting of the bolts during the sliding, which occurs just by means of vertical and horizontal translations. Therefore, Solution B is aimed at solving the issues that occurred in the previous one: the goal is achieved by substituting the pin connection with a bolted connection made with a T-stub and a C-shaped profile and by introducing curved slotted holes in the friction plates, instead of the crossed slotted holes. Even though this solution provides better performance, some weaknesses are highlighted, such as the inadequate stiffness of the top bolted connection (T-stub and C-shaped profile) which is also responsible for the shifting of the centre of rotation during the analysis. The third proposed solution is thus conceived by introducing in the system perfobond connectors and a reduced middle cross-section of the T-stub which resembles the dog-bone-shaped beam ends of steel structures. Solution C is effective in solving the weaknesses still present in Solution B and also allows to experience no significant damage to all elements that constitute the connection device.

Acknowledgements

The authors want to thank the company SICILFERRO TORRENOVESE s.r.l. (Italy) for the economic support.

References

Ballarini, R., La Mendola, L., Le, J., Monaco, A. 2017. Computational study of failure of hybrid steel trussed concrete beams. J. Struct. Eng. ASCE, 143(8): 04017060.

CEB-FIB. 2010, fib Model Code 2010. Comité Euro-International du Béton.

Colajanni, P., La Mendola, L., Monaco, A. 2017. Experimental Investigation on the Shear Response of Precast Steel-Concrete Trussed Beams. J. Struct. Eng. ASCE, 143(1):04016156.

Colajanni, P., La Mendola, L., Monaco, A. 2018. Stress transfer and failure mechanisms in steel-concrete trussed beams: Experimental investigation on slab-thick and full-thick beams. Constr. Build. Mater. 161(1):267-281.

Colajanni, P., La Mendola, L., Monaco, A., Pagnotta, S. (inventors). Seismic dissipation system for building structures. Patent n. 102019000016742, 2019.

Colajanni, P., La Mendola, L., Monaco, A., Pagnotta, S. 2020. Dissipative connections of rc frames with prefabricated steel-trussed-concrete beams. Ingegneria Sismica, 37(1):51-63.

Colajanni, P., La Mendola, L., Monaco, A., Pagnotta, S. 2021a. Design of RC joints equipped with hybrid trussed beams and friction dampers, Engineering Structures, 227:111442.

Colajanni, P., La Mendola, L., Monaco, A., Pagnotta, S. 2021b. Seismic Performance of Earthquake-Resilient RC Frames Made with HSTC Beams and Friction Damper Devices. Journal of Earthquake Engineering, 1-27.

Colajanni, P., La Mendola, L., Monaco, A., Spinella, N. 2016. Cyclic behavior of composite truss beam-to-RC column joints in MRFS. Key Engineering Materials, 711:681-689.

D'Aniello, M., Cassiano, D., Landolfo, R. 2017. Simplified criteria for finite element modelling of European preloadable bolts. Steel and Composite Structures 24 (6):643-658.

Eligehausen, R., Popov, E.P., Bertero, V.V. 1983. Local bond stress-slip relationships of deformed bars under generalized excitations. UCB/EERC-83/23, College of Engineering, University of California, Berkeley, CA.

Eurocode 3 - EN 1993:1-8. 2005. Design of steel structures – Part 1-8: design of joints. CEN

Ferrante Cavallaro G., Latour M., Francavilla A., Piluso V., Rizzano G. 2018, "Standardised friction damper bolt assemblies time-related relaxation and installed tension variability". Journal of Constructional Steel Research, 141:145-155

Francavilla, A. B., Latour, M., Piluso, V., Rizzano, G. 2018. Design of Full-Strength Full-Ductility Extended End-Plate Beam-to-Column Joints. Journal of Constructional Steel Research, 148,77–96.

Monaco, A. 2016. Numerical prediction of the shear response of semi-prefabricated steel-concrete trussed beams. Construction and Building Materials, 124:462-474.

Saenz, L. P. 1964. Discussion of "Equation for the stress-strain curve of concrete," by Desayi & Krishnan. ACI Struct. Journal 61 (9):1229-1235.

Tartaglia, R., D'Aniello, M., Rassati, G.A., Swanson, J., Landolfo, R. 2017. Influence of Composite Slab on the Nonlinear Response of Extended End-Plate Beam-to-Column Joints. Key Engineering Materials 763,818–25.

Yun, X., Gardner, L. 2017. Stress-strain curves for hot-rolled steels. Journal of Constructional Steel Research 133:36-46.